Simulation and Research on Three-Phase Parallel PFC with Feed-Forward Compensation

Chen Qian，He Mingzhi，Trillion Q.Zheng
School of Electrical Engineering，Beijing Jiaotong University
100044，Beijing China
E-mail：chenqian05291148@126.com http://www.126.com

Abstract: - In order to enhance the power factor and minimize the complexity of control strategy, the analysis of a novel three-phase parallel power factor correction with feed-forward compensation is presented. According to the working principle of the topology, hysteresis current control strategy has been proposed for the bi-boost crossing converter. The simulation results verify the stability of the system. As a result, the time sequence of the system is so simple that the switches can be easily controlled to achieve stable output voltage, ideal power factor and current harmonic, while only twenty percents of the total power passes through the Boost converter. In order to achieve ideal power factor and low current harmonic, the output power should be constant.

Key-Words: - Three-phase power factor correction; Feed-forward compensation; Low current harmonic; Hysteresis current control; Bi-boost crossing converter; Constant-power load

1 Introduction

Owing to the simplicity and reliability of the topology, three-phase uncontrolled rectifier has been widely used in high-power applications. However, three-phase uncontrolled rectifier brings nonlinear and transfuses harmonic current into grid [1-3]. It's necessary to restrict harmonic current and power factor to a certain range as electrical standards.

Both of passive filter and active filter can restrain current harmonic and enhance the power factor. Passive filters made of LC series circuits are simple in working principle and topology. The conception of three-phase rectifier with near sinusoidal input current (RNSIC) can achieve ideal power factor and low current harmonic only by additional inductors and capacitors. But the value of inductors and capacitors are unrealistic, further more RNSIC demands for a constant load [4-5]. Multi-pulse rectifier realize low cost and high efficiency without control system, but the harmonic of input current remains high [6-8]. Active filter consisting of voltage-source or current-source PWM (Pulse-Width Modulation) inverters can overcome the drawbacks of passive filter. For example, PWM rectifier and APFC (Active Power Factor Correction) are both active filters. Compared with passive filter, active filter is more competitive [9]. Although the input current of PWM rectifier is near sinusoidal, it has several drawbacks as follows [10-12]: complex control strategy, high cost and high switching losses, which is serious in high power system. Presently, the technique of the three-phase APFC isn't as mature as the single phase, which is recognized by many scholars. Three-phase parallel PFC with feed-forward compensation lack deeply research on working principle and control system, even if it has been put forward by scholars [13-16].

In this paper, working principle is deeply analyzed and then theoretical model is established. According to the theoretical model, a new control scheme has been put forward and the performance characteristic of this topology has been discussed. Furthermore, simulation model has been built to verify the accuracy and feasibility of the new control scheme.

2 Analysis of Working Principle

The topology of three-phase parallel PFC with feed-forward compensation which includes main and subordinate rectifiers is shown in Fig.1. The main rectifier is a common three-phase uncontrolled rectifier, while the subordinate rectifier is a bi-boost crossing APFC circuit. S_a、S_b、S_c are bi-directional switches. The nomenclature used in Fig.1 is reported here below:

I_{am}, I_{bm}, I_{cm} = Phase currents of main rectifier

I_{aa}, I_{ba}, I_{ca} = Phase currents of subordinate rectifier

I_a, I_b, I_c = Sum of phase currents of main and subordinate rectifier.

I_r = Output current of subordinate rectifier

I_m = Output current of main rectifier

I_s = Output current of bi-boost crossing converter

I_o = Load current

V_a = Output voltage of subordinate rectifier

V_m = Output voltage of main rectifier

V_0 = Output voltage of this topology

V_a = Input voltage of branch 1 and branch 2

U_{32} = Output voltage of branch 1

U_{14} = Output voltage of branch 2

U_{32} = Voltage between nodes ② and ③

U_{14} = Voltage between nodes ① and ④

U_{34} = Voltage between nodes ③ and ④

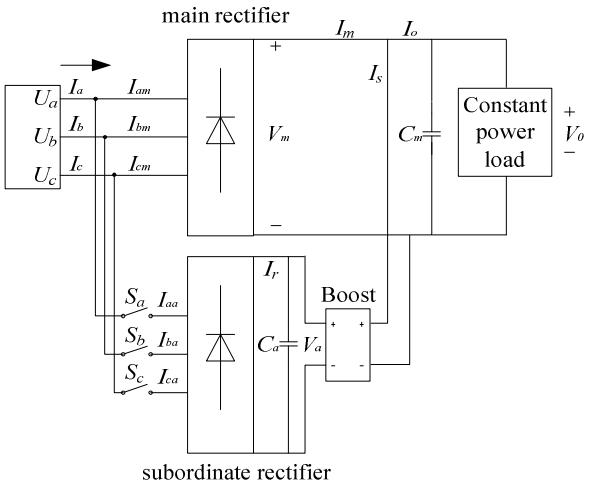

(a) Topology of main circuit

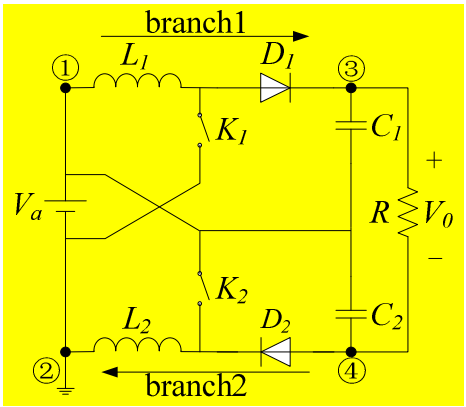

(b) Topology of bi-boost crossing converter

Fig.1 Topology of three-phase parallel PFC with feed-forward compensation

Bi-boost crossing converter whose symmetry boost converters are parallel in input terminal and serial in output terminal is shown in Fig.1 (b) [17]. The symmetry boost converters are independent with each other. If D_1, D_2 are the duty cycles of switches K_1 and K_2 respectively.

$$U_{32} = \frac{1}{1-D_1} V_a \quad (1)$$

$$U_{14} = \frac{1}{1-D_2} V_a \quad (2)$$

$$V_0 = U_{34} = \frac{1}{1-D_1} V_a + \frac{D_2}{1-D_2} V_a \quad (3)$$

If $D_1 = D_2 = D$,

$$V_0 = \frac{1+D}{1-D} V_a \quad (4)$$

Compared with the normal boost converter, bi-boost crossing converter has the following advantages:

1) Wider adjustable range of output voltage;
2) The current stress of switch is half of the one of normal boost converter, the voltage stress is 1/(1+D) of the one of normal boost converter;
3) Two branches can be controlled independently to restrain the circulation.

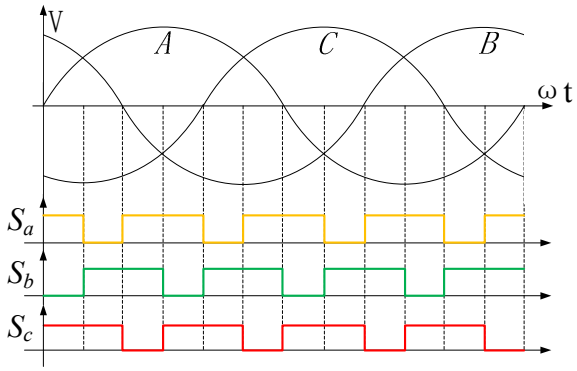

Fig.2 Sequence of S_a、S_b、S_c during a period

A period is divided into twelve intervals. The sequences of S_a、S_b、S_c during a period are shown in Fig.2. The working phase of main and subordinate rectifier and formulae of I_a、I_b、I_c are shown in Table 1. The working phase of main rectifier is the one whose absolute value is larger between the two phases with the same polarity and the one with the reverse polarity, while the working phase of subordinate rectifier is the one whose absolute value is smaller between the two phases with the same polarity and the one with the reverse polarity. For example, during $(0, \pi/6)$ interval, the working phase of main rectifier is phase B and C while the working phase of subordinate rectifier are phase A and C by controlling S_a and S_c.

Table 1 Working phase of main and subordinate rectifier and formulas of I_a、I_b、I_c during a period

	$(0,\frac{\pi}{6})$	$(\frac{\pi}{6},\frac{2\pi}{6})$	$(\frac{2\pi}{6},\frac{3\pi}{6})$	$(\frac{3\pi}{6},\frac{4\pi}{6})$	$(\frac{4\pi}{6},\frac{5\pi}{6})$	$(\frac{5\pi}{6},\frac{6\pi}{6})$
Working phase of main rectifier	BC	AC	AC	AB	AB	CB
Working phase of subordinate rectifier	AC	BC	AB	AC	CB	AB
I_a	I_{aa}	I_{am}	$I_{aa}+I_{am}$	$I_{aa}+I_{am}$	I_{am}	I_{aa}
I_b	I_{bm}	I_{ba}	I_{ba}	I_{bm}	$I_{bm}+I_{ba}$	$I_{bm}+I_{ba}$
I_c	$I_{cm}+I_{ca}$	$I_{cm}+I_{ca}$	I_{cm}	I_{ca}	I_{ca}	I_{cm}
	$(\frac{6\pi}{6},\frac{7\pi}{6})$	$(\frac{7\pi}{6},\frac{8\pi}{6})$	$(\frac{8\pi}{6},\frac{9\pi}{6})$	$(\frac{9\pi}{6},\frac{10\pi}{6})$	$(\frac{10\pi}{6},\frac{11\pi}{6})$	$(\frac{11\pi}{6},\frac{12\pi}{6})$
Working phase of main rectifier	CB	CA	CA	BA	BA	BC
Working phase of subordinate rectifier	CA	CB	BA	CA	BC	BA
I_a	I_{aa}	I_{am}	$I_{aa}+I_{am}$	$I_{aa}+I_{am}$	I_{am}	I_{aa}
I_b	I_{bm}	I_{ba}	I_{ba}	I_{bm}	$I_{bm}+I_{ba}$	$I_{bm}+I_{ba}$
I_c	$I_{cm}+I_{ca}$	$I_{cm}+I_{ca}$	I_{cm}	I_{ca}	I_{ca}	I_{cm}

The current waveform I_a is shown in Fig.3. The missing current during $(0,\pi/6)$, $(5\pi/6,7\pi/6)$, $(11\pi/6,2\pi)$ makes I_a distort. If the missing current is compensated, the harmonic of I_a will reduce obviously. So the bi-boost crossing converter should be controlled to compensate the missing current during $(0,\pi/6)$, $(5\pi/6,7\pi/6)$, $(11\pi/6,2\pi)$ and improve the current during $(\pi/6,5\pi/6)$, $(7\pi/6,11\pi/6)$. It's the same with phase B and C.

Based on the above analysis, I_r is in phase with V_a, which is presented in Fig.4.

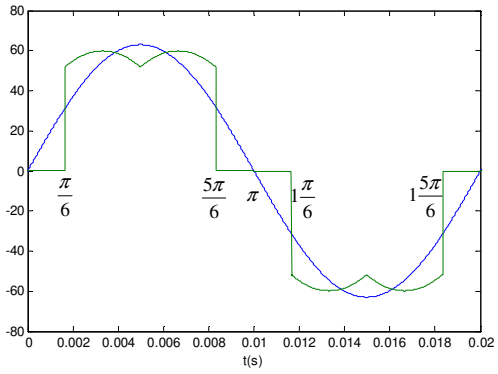

(a) The waveform of phase current I_a

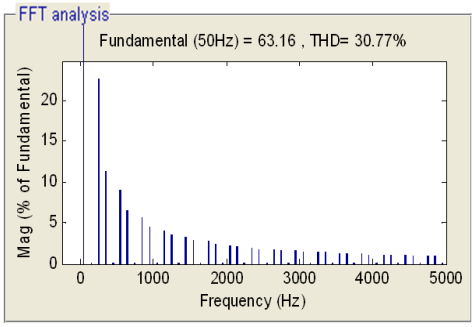

(b) The frequency spectrum of I_a

Fig.3 Phase current waveforms and frequency spectrum of three-phase uncontrolled rectifier without capacitor

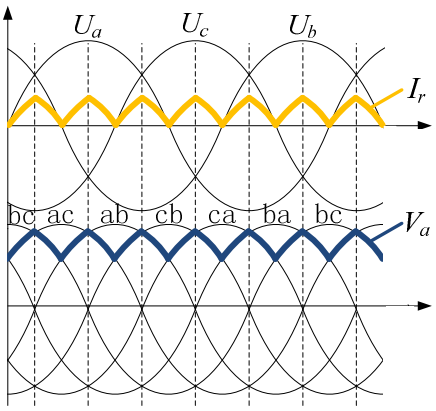

Fig.4 Ideal waveforms of I_r and V_a

3 Harmonic Analysis of Input Current

Supposing the peak value of phase voltage is V and the output power is P. The following harmonic analysis is based on the constant power load (just like DC-DC converter).

Three phase voltages are

$$\begin{cases} U_a = V\sin(\omega t) \\ U_b = V\sin(\omega t + 2\pi/3) \\ U_c = V\sin(\omega t + 4\pi/3) \end{cases} \quad (5)$$

If the power factor is unity, three phase input currents are

$$\begin{cases} I_a = k\sin(\omega t) \\ I_b = k\sin(\omega t + 2\pi/3) \\ I_c = k\sin(\omega t + 4\pi/3) \end{cases} \quad (6)$$

For the output power P

$$P = U_a I_a + U_b I_b + U_c I_c = 1.5Vk, \quad k = \frac{P}{1.5V} \tag{7}$$

So

$$\begin{cases} I_a = \dfrac{P}{1.5V}\sin(\omega t) \\ I_b = \dfrac{P}{1.5V}\sin(\omega t + 2\pi/3) \\ I_c = \dfrac{P}{1.5V}\sin(\omega t + 4\pi/3) \end{cases} \quad (8)$$

If the filter capacitors C_m and C_a are ignored and the switching frequency can be as high as possible, the output voltage of subordinate rectifier is close to six-pulse. Since the frequency of I_r is six times as power frequency, the current harmonic is only analyzed during interval $(0,\pi/3)$. The relationship of phase currents is shown in Fig.5 during this interval. The reference direction of input current has been marked in Fig.1.

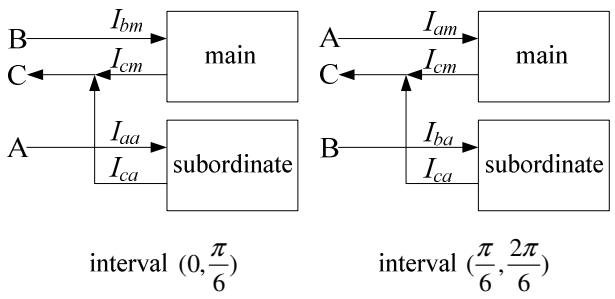

Fig.5 Relationship of phase currents during $(0,\pi/3)$

（1）Interval $(0,\pi/6)$

The working phases of main rectifier are phase B and C, while phase A and C are the working phases of subordinate rectifier.

$$V_0 = V_{bc} = \sqrt{3}V\sin(\omega t + \pi/2) \quad (9)$$

$$V_a = V_{ac} = \sqrt{3}V\sin(\omega t + \pi/6) \quad (10)$$

In order to compensate the missing current and achieve unity power factor during this interval,

$$I_a = I_{aa} = \frac{P}{1.5V}\sin(\omega t) \quad (11)$$

Due to the power conservation principle, the relationship between I_r and I_s is

$$I_s = \frac{V_a I_r}{V_0} = \frac{P}{\sqrt{3}V} \times \frac{\sin(\omega t)\sin(\omega t + \frac{\pi}{6})}{\sin(\frac{\pi}{3})\sin(\omega t + \frac{\pi}{2})} \tag{12}$$

$$I_b = I_{bm} = \frac{P}{V_0} - I_s = \frac{P}{1.5V}\sin(\omega t + \frac{2}{3}\pi) \tag{13}$$

$$I_c = I_{cm} + I_{ca} = -I_{bm} - I_{aa} = \frac{P}{1.5V}\sin(\omega t - \frac{2\pi}{3}) \tag{14}$$

（2）Interval $(\pi/6,\pi/3)$

The working phases of main rectifier are phase A and C, while phase B and C are working phases of subordinate rectifier.

$$V_0 = V_{ac} = \sqrt{3}V\sin(\omega t + \frac{\pi}{6}) \quad (15)$$

$$V_a = V_{bc} = \sqrt{3}V\sin(\omega t + \frac{\pi}{2}) \quad (16)$$

In order to compensate the missing current during this interval,

$$I_b = I_{ba} = \frac{P}{1.5V}\sin(\omega t + \frac{2\pi}{3}) \quad (17)$$

Due to the power conservation principle, the relationship between I_r and I_s is

$$I_s = \frac{V_a I_r}{V_0} = \frac{P}{\sqrt{3}V} \times \frac{\sin(\omega t + \frac{2\pi}{3})\sin(\omega t + \frac{\pi}{2})}{\sin(\frac{\pi}{3})\sin(\omega t + \frac{\pi}{6})} \tag{18}$$

$$I_a = I_{am} = \frac{P}{V_0} - I_s = \frac{P}{1.5V}\sin(\omega t) \tag{19}$$

$$I_c = I_{cm} + I_{ca} = -I_{am} - I_{ba} = \frac{P}{1.5V}\sin(\omega t - \frac{2\pi}{3}) \tag{20}$$

The formula of input current is the same during the other intervals. According to the analysis above, when (11) and (17) is satisfied, I_a, I_b, I_c will be

sinusoidal and the power factor will be unity if the load is constant-power, the filter capacitors C_m and C_a are ignored and the switching frequency is as high as possible.

Actually the switching frequency can't be as high as possible, so the filter capacitors C_a and C_m should be considered. The formulae of phase A current I_a are shown as follows.

Intervals $(0,\pi/6)$, $(\pi,7\pi/6)$

$$I_a=\frac{P}{1.5V}\sin(\omega t)+\sqrt{3}V\cdot\omega C_a\cos(\omega t+\frac{\pi}{6}) \tag{21}$$

Intervals $(\pi/6,\pi/3)$, $(7\pi/6,8\pi/6)$

$$I_a=\frac{P}{1.5V}\sin(\omega t)+\sqrt{3}V\cdot\omega C_m\cos(\omega t+\frac{\pi}{6}) \tag{22}$$

Intervals $(\pi/3,\pi/2)$, $(4\pi/3,3\pi/2)$

$$I_a=\frac{P}{1.5V}\sin(\omega t)+\sqrt{3}V[\omega C_m\cos(\omega t+\frac{\pi}{6}) +\omega C_a\cos(\omega t-\frac{\pi}{6})] \tag{23}$$

Intervals $(\pi/2,2\pi/3)$, $(3\pi/2,5\pi/3)$

$$I_a=\frac{P}{1.5V}\sin(\omega t)+\sqrt{3}V[\omega C_m\cos(\omega t-\frac{\pi}{6}) +\omega C_a\cos(\omega t+\frac{\pi}{6})] \tag{24}$$

Intervals $(2\pi/3,5\pi/6)$, $(5\pi/3,11\pi/6)$

$$I_a=\frac{P}{1.5V}\sin(\omega t)+\sqrt{3}V\cdot\omega C_m\cos(\omega t-\frac{\pi}{6}) \tag{25}$$

Intervals $(5\pi/6,\pi)$, $(11\pi/6,2\pi)$

$$I_a=\frac{P}{1.5V}\sin(\omega t)+\sqrt{3}V\cdot\omega C_a\cos(\omega t-\frac{\pi}{6}) \tag{26}$$

It's concluded that the harmonic current is concerned with gross power P, peak value of phase voltage V, angular frequency ω and filter capacitors C_m and C_a if the filter capacitors C_a and C_m are considered.

4 Principle of Control System

It is only needed to control the switch S_a, S_b, S_c, K_1 and K_2 to achieve ideal power factor and low harmonic current. The system control scheme of subordinate rectifier is shown in Fig.6. In order to achieve ideal power factor and low harmonic current, the average value of I_{s1}, I_{s2} and the waveforms of I_{r+}, I_{r-} should be controlled by detecting the input current I_{r+} and I_{r-}, output current I_{s1} and I_{s2} and three phase voltages.

The time sequence of S_a, S_b and S_c which is decided by the phase voltage is shown in Fig.2. Commonly the AC-DC switched converter has three control methods: peak current control, hysteresis current control and average current control. The advantages of hysteresis current control are proposed as follows: simple control, quick dynamic response of current, excellent disturbances attenuation performances and robustness. So the hysteresis current control scheme which is represented in Fig.7 has been chosen for this novel APFC topology. The values of I_{r+} and I_{s1} are the current feedbacks for K_1, while the values of I_{r-} and I_{s2} are the current feedbacks for K_2. So K_1 and K_2 are controlled independently, but both of them choose $I_{r(wave)}$ as reference phase current. The circulation will be avoided by controlling K_1 and K_2 independently.

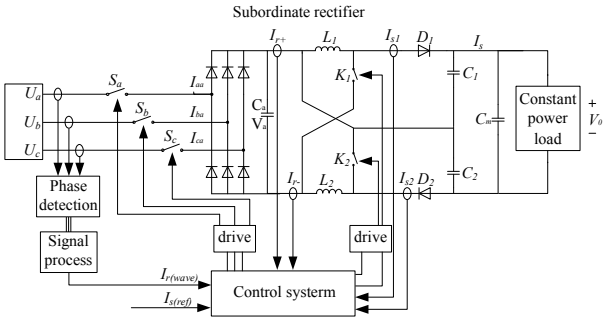

Fig.6 System control scheme of three-phase parallel PFC with feed-forward compensation

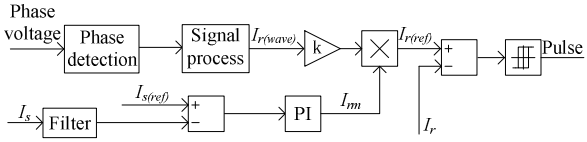

Fig.7 Hysteresis current control scheme of three-phase parallel PFC with feed-forward compensation

The control scheme to implement three-phase parallel PFC with feed-forward compensation should focus on two points:

1) The load power is constant;

2) Compensate the missing current in zero crossing interval of each phase and keep the power factor unity. For example, during $(0,\pi/6)$, $I_{r+}=I_{r-}=P\sin(\omega t)/1.5V$.

The main rectifier which is a three-phase uncontrolled rectifier is equivalent as a voltage

source, while the subordinate rectifier whose output current is controlled is equivalent as a current source. The output voltage of this novel APFC topology is equal to the voltage of the equivalent voltage source. If the load power is constant, the load current I_0 will be constant. The missing current can be compensated by controlling I_s and I_r.

The power of subordinate rectifier is

$$P_s = \frac{6}{\pi}\int_0^{\frac{\pi}{6}} \frac{P}{1.5V}\sin(\omega t)\cdot\sqrt{3}V\sin(\omega t+\frac{\pi}{6})d\omega t$$
$$= V_m \times I_s = 0.224P \quad (27)$$

The total output power is P, and the power of main rectifier is

$$P_m = V_m \times I_m = P - 0.224P = 0.776P \quad (28)$$

According to (27) and (28)

$$\frac{I_m}{I_s} = \frac{97}{28} \quad (29)$$

If (29) is valid in this system and I_r is able to track the phase of $I_{r(wave)}$, ideal power factor and low harmonic current will be achieved.

The relationship between $I_{r(wave)}$ and V_a is shown in Fig.4. $I_{r(wave)}$ is decided by phase voltage. $I_{s(ref)}$ is the reference current of outer current loop. According to (29), $I_{s(ref)}=28I_m/97$. The reference current of inductance $I_{r(ref)}$ is the product of $kI_{r(wave)}$ and the output of the PI controller of the current outer loop. The principle of hysteresis current control is shown in Fig.8. The upper limit of hysteresis loop is defined as $I_{r(ref)}+\Delta h$ and the lower limit is $I_{r(ref)}-\Delta h$. If $I_r>I_{r(ref)}+\Delta h$, switch will be off and the inductance current will decrease, otherwise switch will be on and the inductance current will increase. The inductance current fluctuate near the reference current $I_{r(ref)}$ by controlling K_1 and K_2. How to choose Δh for the control system is important, because it's concerned with current harmonic. In order to improve the switching characteristic of K_1 and K_2, the sample value of inductance current should be filtered.

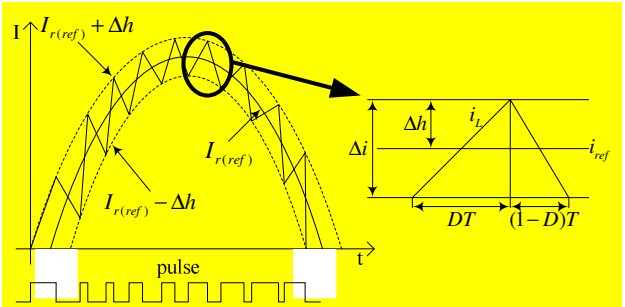

Fig.8 Principle of hysteresis current control

5 Simulation Results

The MATLAB/Simulink simulation model consists of a three phase voltage source (with peak phase voltage V=311V and f=50Hz) and a three-phase parallel PFC with feed-forward compensation. The output power is 30 KW, and the maximum switching frequency is 20 KHz. For the inductors L, we have adopted the value of 0.5mH. The filter capacitor C_m is 40uF, and C_a is 20uF. For the outer current loop of control system, the scale factor K_p=0.015 and the integral factor K_i=5. The scale factor of phase control loop K is 0.1, and the hysteresis width Δh is 3.

The phase current I_a of normal three-phase uncontrolled rectifier, theoretical model and simulation model with hysteresis current control are presented in Fig.9, Fig.10 and Fig.11 respectively. With the filter whose cut-off frequency is 5 KHz, the frequency spectrum of I_a is shown in Fig.12. From theoretical model, the THD (Total Harmonic Distortion) of I_a is 4.65%, while the THD of I_a is 10.84% from simulation model. Compared with 31.2% of normal three-phase uncontrolled rectifier, THD has reduced obviously. The reason why the THD of simulation is higher than the theoretical THD is as follows: the theoretical I_s and I_m are continuous, while I_s and I_m from the simulation model are pulsing, which will generate additional higher harmonic. So from the simulation model, the THD of I_a reduces to 5.86% with the filter whose cut-off frequency is 5 KHz.

The current waveforms of I_{aa}, I_{am}, I_a are shown in Fig.13 and the current waveforms of I_a, I_b, I_c are shown in Fig.14. I_{aa} is the compensation of the missing current. In Fig.13, I_a is the sum of I_{aa} and I_{am}. The input and output voltage waveforms of bi-boost crossing converter are shown in Fig.15 and 16. The input current waveforms I_{r+}, I_{r-} of bi-boost crossing converter are shown in Fig.17 (a) and (b). V_a, I_{r+}, I_{r-} from simulation model are coincide with the theoretical results which are shown in Fig.4 and the load voltage V_0 which is equal to the output voltage of main rectifier is six-pulse during a period. Fig.18 shows the voltage and current waveforms of phase A. As is shown in Fig.18, the power factor is 0.9932, which verify the feasibility of this novel APFC topology. Fig.19 shows the waveform of output power, which verifies the premise that the load power keeps constant in the simulation model. In Fig.20, Fig.21and Fig.22, the current stress of switch K_1 and K_2 is half of the one of normal boost converter, the voltage stress of switch K_1 and K_2 is $1/(1+D)$ of the one of normal boost converter, which is coincide with the analysis mentioned in section 2.

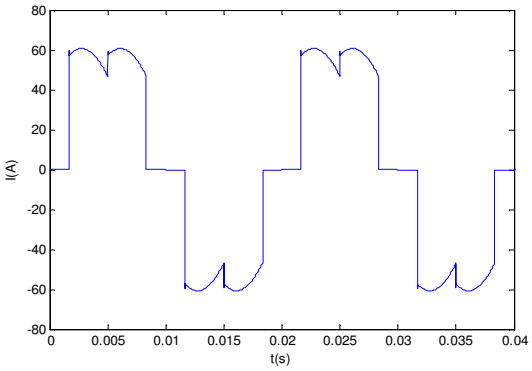

(a) The waveform of phase current I_a

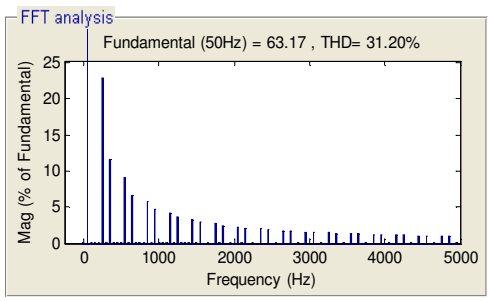

(b) The frequency spectrum of I_a

Fig.9 I_a and frequency spectrum of normal three-phase uncontrolled rectifier

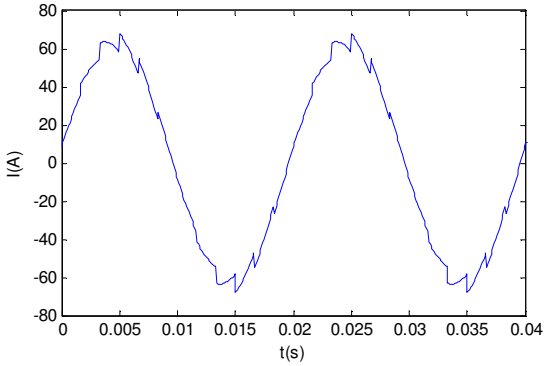

(a) The waveform of phase current I_a

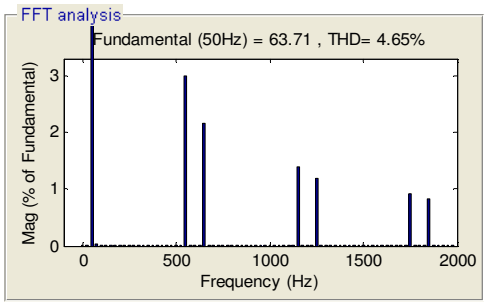

(b) The frequency spectrum of I_a

Fig.10 I_a and frequency spectrum from theoretical model under hysteresis current control

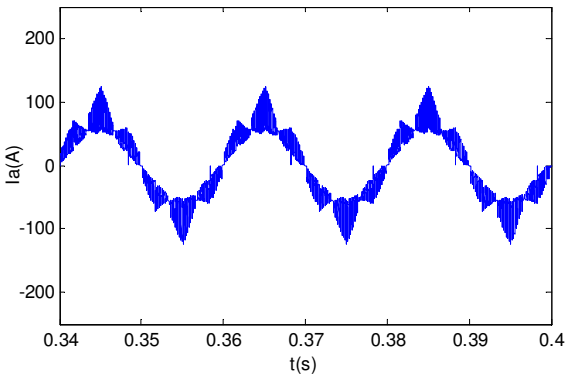

(a) The waveform of phase current I_a

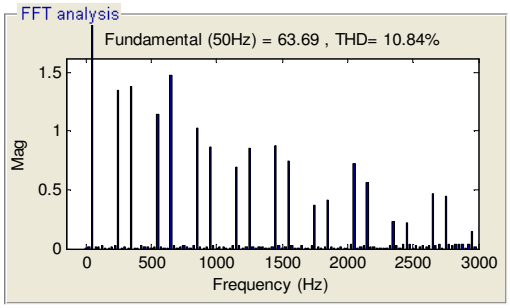

(b) The frequency spectrum of I_a

Fig.11 I_a and frequency spectrum from simulation model under hysteresis current control

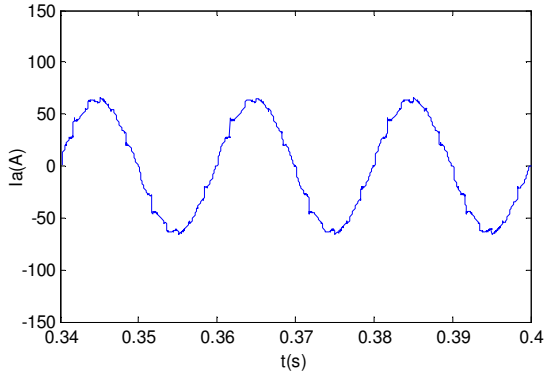

(a) The waveform of phase current I_a

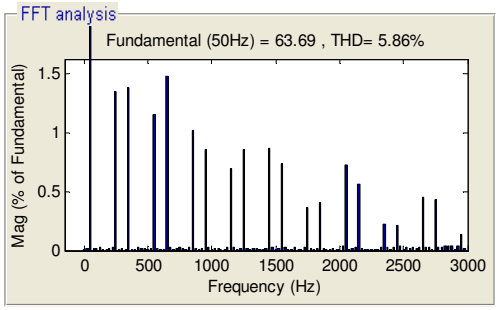

(b) The frequency spectrum of I_a

Fig.12 I_a and frequency spectrum from simulation model with filter under hysteresis current control

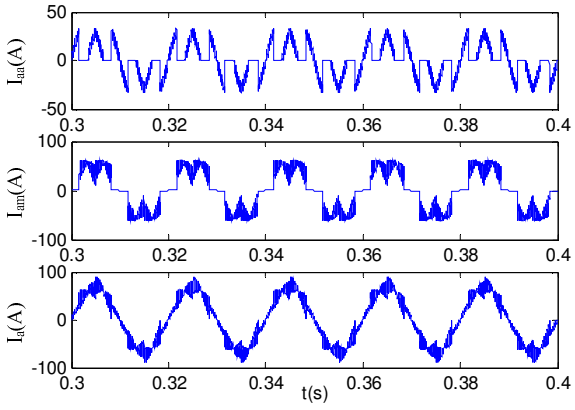

Fig.13 Current waveforms of I_{aa}、I_{am}、I_a

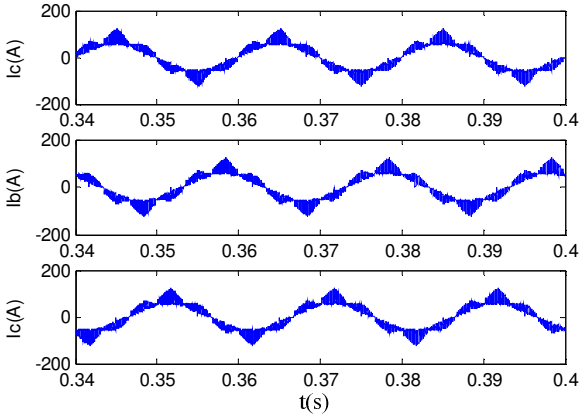

Fig.14 Current waveforms of I_a、I_b、I_c

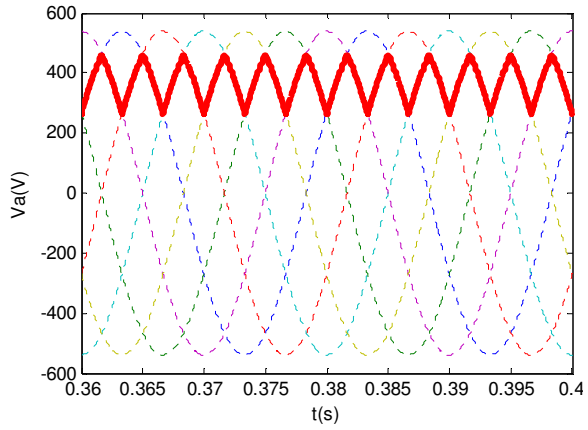

Fig.15 Voltage waveform of V_a

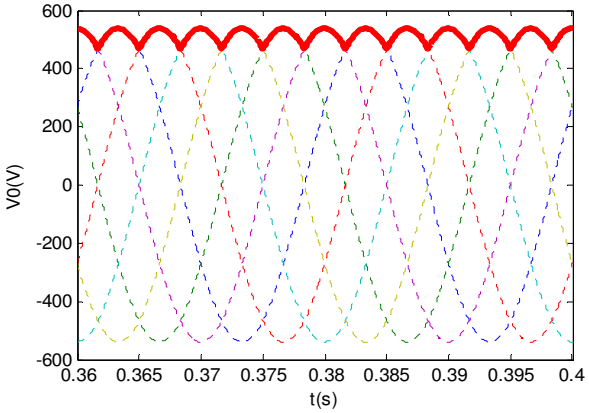

Fig.16 Voltage waveform of V_0

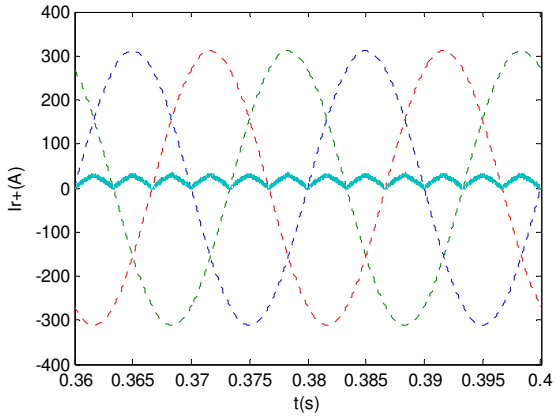

(a) Current waveform of I_{r+}

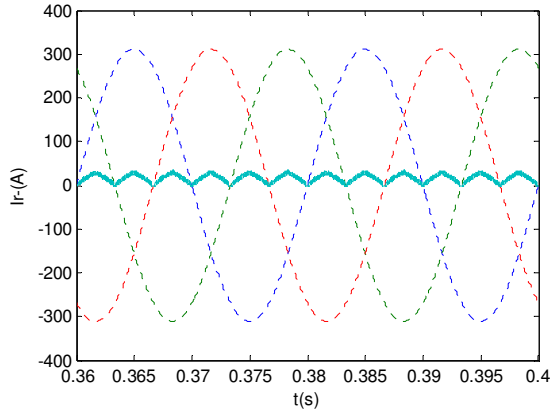

(b) Current waveform of I_{r-}

Fig.17 Input current waveform of Boost circuit

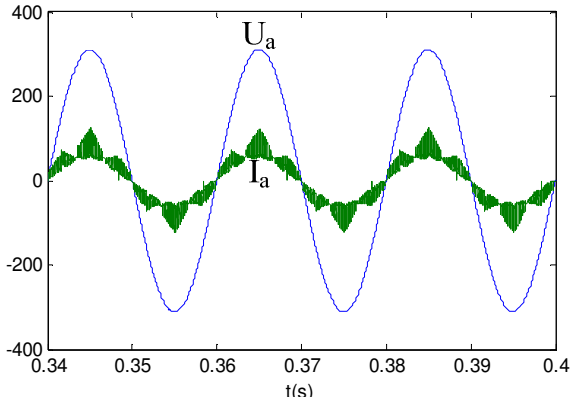

Fig.18 Voltage and current waveforms of phase A

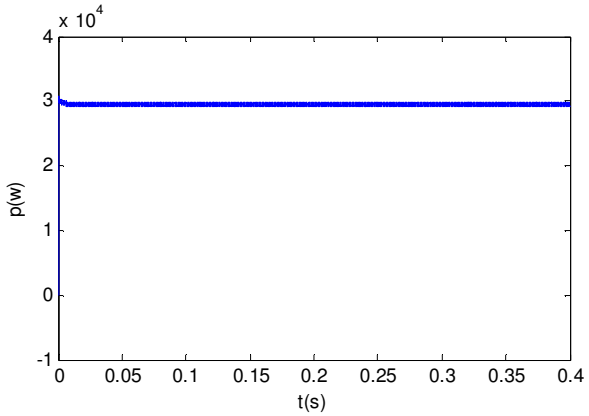

Fig.19 Waveform of output power

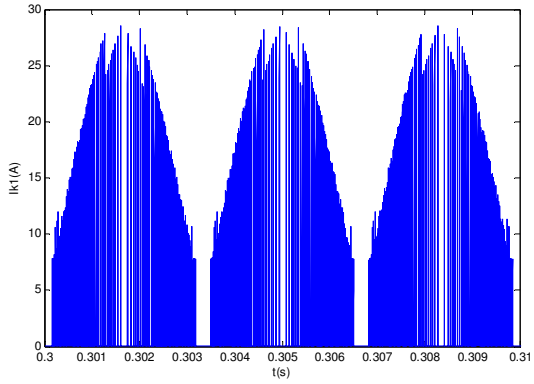

(a) Current stress of switch K_1

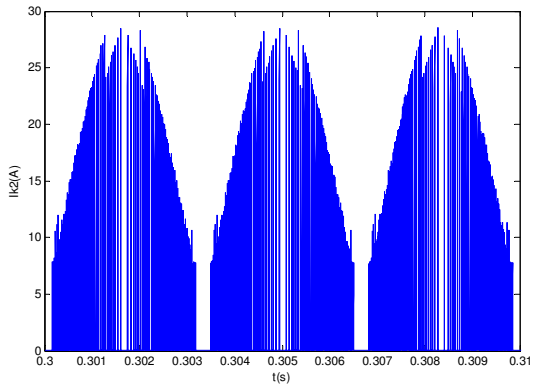

(b) Current stress of switch K_2

Fig.20 Current stress of switch of bi-boost crossing converter

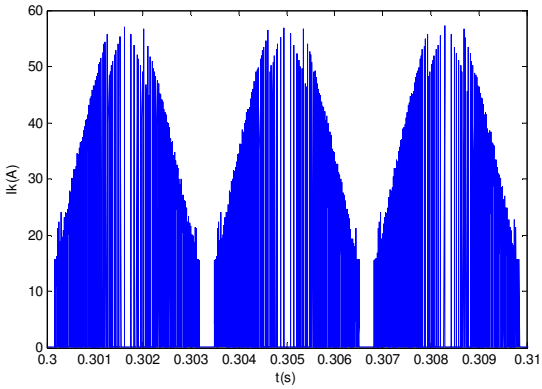

Fig.21 Current stress of switch of normal boost converter

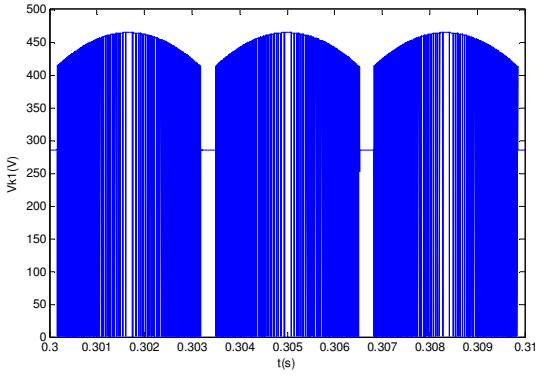

(a) Voltage stress of switch K_1

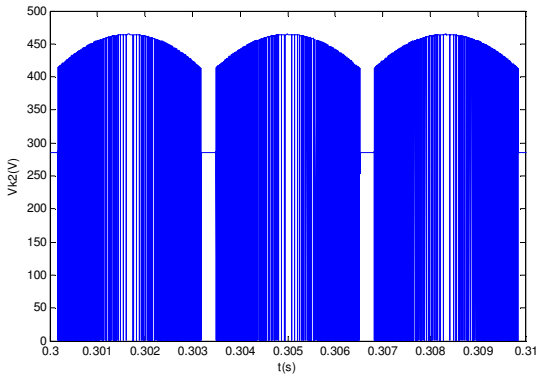

(b) Voltage stress of switch K_2

Fig.22 Voltage stress of switch

6 Conclusion

The novel three-phase PFC topology cooperated with the hysteresis control technique has been proposed. It can stabilize the six-pulse dc output voltage, compensate the missing current during intervals $(0,\pi/6)$, $(5\pi/6,7\pi/6)$, $(11\pi/6,2\pi)$ in a period and improve the other two phase current waveforms during the same interval. The theoretical analysis and the simulation results have proved the merits of small current THD and high power factor. However, when the load power has been changed heavily, the power factor and current THD will get worse, and the DC voltage is not adjustable. Approximately twenty percent of power goes through the boost converter and the bi-boost crossing converter can reduce the voltage and current stress of switch. Therefore, the lower power components can be chosen, which reduce the cost and improve the efficiency of the system. The novel APFC topology is suitable for the applications as follows:

1) Strict with power factor;

2) Output power is constant.

In total, the novel APFC topology has wide application prospects.

References:

[1] Zhang Zheyu, Zou Xudong, Wu Zhenxing et al., *Analysis on Harmonic Current of Three-phase Bridge Uncontrolled Rectifier*, IEEE Power and Energy Engineering Conference, Wuhan, China, 2010, pp.1-4.

[2] Sakui, M., Fujita, H., Shioya, M.., *A method for calculating harmonic currents of a three-phase bridge uncontrolled rectifier with DC filter*, IEEE Transactions on Industrial Electronics, Vol.36, No.3, 1999, pp.434-440.

[3] Li Mingshui, Wan Jianru, Li Guangye et al,

Research on power feedforward control strategy of PWM rectifier, Power Electronics Systems and Applications, Tianjin, China, 2011, pp.1-6.

[4] Chen Zhong, Zhu Yin-yu, Luo Ying-peng, *Three-Phase Rectifier With Near-Sinusoidal Input Currents and LC Filters Connected on the AC Side*, Transactions of China Electrotechnical Society, Vol.24, No.11, 2009, pp.108-113.

[5] Chen Zhong, Zhu Yin-yu, Qiu Yan, et al, *Analysis and Design of Three-phase Rectifier With Near-sinusoidal Input Currents*, Proceedings of the CSEE, Vol.29, No.36, 2009, pp.29-34.

[6] Burgos R P, Uan-Zo-li A, Lacaux F, et al, *Analysis of new step-up and step-down 18-pulse direct asymmetric autotransformer rectifiers*, IEEE Industry Applications Conference, Hong Kong, China, Vol.1, 2005, pp.145-152.

[7] Chen Peng, Li Xiaofan, Xiong Zhaochun, et al, *A 12-pulse rectifier with an auxiliary circuit*, Proceedings of the CSEE, Vol.26, No.23, 2006, pp.163-166.

[8] Singh B, Bhuvaneswari G, Garg V, *T-connected autotransformer-based 24-pulse AC-DC converter for variable frequency induction motor drives*, IEEE Transaction on Energy Conversion, Vol.21, No.3, 2006, pp.663-672.

[9] Wang Zhaoan, Yang Jun, Liu Jinjun, et al, *Harmonic suppression and Reactive power compensation*, Beijing: Machine Press, 2005.

[10] Divya, E., Gnanavadivel, J.. *Harmonic elimination in three phase PWM rectifier using FPGA control*, Emerging Trends in Electrical and Computer Technology Conference, Sivakasi, India, 2011, pp.436-441.

[11] Hyunjae Yoo, Kim, J.-H., Seung-Ki Sul, *Sensorless Operation of a PWM Rectifier for a Distributed Generation*, IEEE Transactions on Power Electronics, Vol.22, No.3, 2007, pp.1014-1018.

[12] Dae-Woong Chung, Seung-Ki Sul., *Minimum-loss strategy for three-phase PWM rectifier*, IEEE Transactions on Industrial Electronics, Vol.46, No.3, 1999, pp.517-526.

[13] Y.F. Wang, *Boost converter with lower inter-phase rectifier parallel compensating three-phase power factor correction*, PCT/CN/02/00828.

[14] Y.F. Wang, Bingxin Wang, Zian Zhu, *A Voltage-Adjustable Three-Phase Rectifier with Constant Power Flow*, Applied Power Electronics Conference and Exposition, 2008, pp.1372-1377.

[15] Y.F. Wang, *Blocked Phase Current Patching Three-phase Rectifier and Motor Driver with Energy Feedback*, PCIM China, 2009, pp.168-173.

[16] Y.F. Wang, *Three-phase parallel PFC with feed-forward compensation*: China, 01140014.5. 2003-05-28.

[17] Yi. Li, *DC-DC Circuit with symmetrical crossing structure*: China, 101867314A. 2010-10-20.